

# Predicting lymph node metastasis from primary tumor histology and clinicopathologic factors in colorectal cancer using deep learning

## Authors:

Justin D. Krogue<sup>1\*</sup>, Shekoofeh Azizi<sup>2</sup>, Fraser Tan<sup>1</sup>, Isabelle Flament-Auvigne<sup>3</sup>, Trissia Brown<sup>3</sup>, Markus Plass<sup>4</sup>, Robert Reihls<sup>4</sup>, Heimo Müller<sup>4</sup>, Kurt Zatloukal<sup>4</sup>, Pema Richeson<sup>5</sup>, Greg S. Corrado<sup>1</sup>, Lily H. Peng<sup>1</sup>, Craig H. Mermel<sup>1</sup>, Yun Liu<sup>1</sup>, Po-Hsuan Cameron Chen<sup>1</sup>, Saurabh Gombhar<sup>5</sup>, Thomas Montine<sup>5</sup>, Jeanne Shen<sup>5</sup>, David F. Steiner<sup>1,†</sup>, Ellery Wulczyn<sup>1,†</sup>

## Affiliations:

<sup>1</sup>Google Health, Palo Alto, California, United States of America

<sup>2</sup>Google Research, Brain Team, Toronto, Ontario, Canada

<sup>3</sup>Work done at Google Health via Vituity, Emeryville, CA, United States of America

<sup>4</sup>Medical University of Graz, Graz, Austria

<sup>5</sup>Department of Pathology, Stanford University School of Medicine, Stanford, California, United States of America

<sup>†</sup>Equal contribution

\*Corresponding author: [justin.d.krogue@gmail.com](mailto:justin.d.krogue@gmail.com)

# Supplementary Material

## Supplementary Methods

### Embedding Models

In this work we explored three different models for generating image patch embeddings: Graph-Rise, BiT and SimCLR.

#### Graph-RISE

The Graph-Regularized Image Semantic Embedding (Graph-RISE) model<sup>18</sup> is a large scale image embedding neural network trained on approximately 40M classes from 260M web images. This model has been successfully employed in prior pathology related tasks such as image search<sup>18,19</sup> and generating machine-learned features survival prediction<sup>15</sup>.

#### BiT

The Bit Transfer (BiT) model<sup>20</sup> used in the work is based on ResNet50<sup>22</sup> neural network architecture trained on the publicly available ImageNet<sup>23</sup> dataset.

#### SimCLR

The SimCLR<sup>21</sup> model used in this work was initialized with the ResNet50 BiT model described above and then trained using the SimCLR methodology on a random sample of 50M patches from 10,705 cases (29,018 slides) spanning 32 studies from The Cancer Genome Project (TCGA). This model was trained for 5M steps with a batch size of 1024 with a learning rate of 0.3 and temperature of 0.1, and was trained on V2 TPU.

## Supplementary Tables

### **Supplementary Table S1: Cohort characteristics**

The development set consists of Stages II or III cases with T-categories 3 or 4 from the Medical University of Graz from 1984 to 2007. The temporal validation set consists of Stages II or III with T-categories 3 or 4 cases from the Medical University of Graz from 2008-2013. External validation set 1b consists of Stages I-IV with T-categories 2-4 from Stanford University from 2007-2018. External validation set 1a is a subset of external validation set 1b containing only Stages II or III with T-categories 3 or 4.

**Supplementary Table S2: Pathologist descriptions of machine-learned features**

<b>Feature</b>	<b>Description</b>
<b>1</b>	Predominantly adipose and inflammatory cells with occasional tumor cells
<b>2</b>	Predominantly low grade adenocarcinoma and associated stroma
<b>3</b>	Predominantly moderately differentiated adenocarcinoma and occasional inflammatory and fibrotic stroma
<b>4</b>	Predominantly high grade adenocarcinoma with high tumor:stroma ratio
<b>5</b>	Predominantly low grade to moderately differentiated adenocarcinoma with occasional inflammatory cell infiltrate and intraglandular necrotic debris

**Supplementary Table S3: Performance for LNM prediction using different embedding models to generate features**

AUROC for LNM predictions for logistic regressions containing baseline clinicopathologic variables (age, sex, tumor grade, T-category, lymphatic invasion, venous invasion) and the top-5 machine-learned features from different embedding models. 95% CIs computed via bootstrapping.

Dataset	Embedding Model		
	Graph-RISE	BiT	SimCLR
Temporal validation	0.715 [0.674, 0.753]	0.730 [0.689, 0.766]	0.703 [0.660, 0.740]
External validation 1a	0.740 [0.701, 0.780]	0.737 [0.697, 0.782]	0.737 [0.696, 0.778]
External validation 1b	0.738 [0.705, 0.770]	0.731 [0.698, 0.763]	0.740 [0.706, 0.772]

**Supplementary Table S4: Sensitivity, specificity, PPV, and NPV for each model using optimized threshold.**

The optimized threshold was determined by selecting the value that maximized the harmonic mean of sensitivity and specificity. **Clinical**: baseline clinicopathologic variables (age, sex, tumor grade, T-category, lymphatic invasion, venous invasion). **Clinical + ML**: baseline clinicopathologic variables plus 5 machine-learned features. 95% confidence intervals computed via bootstrapping.

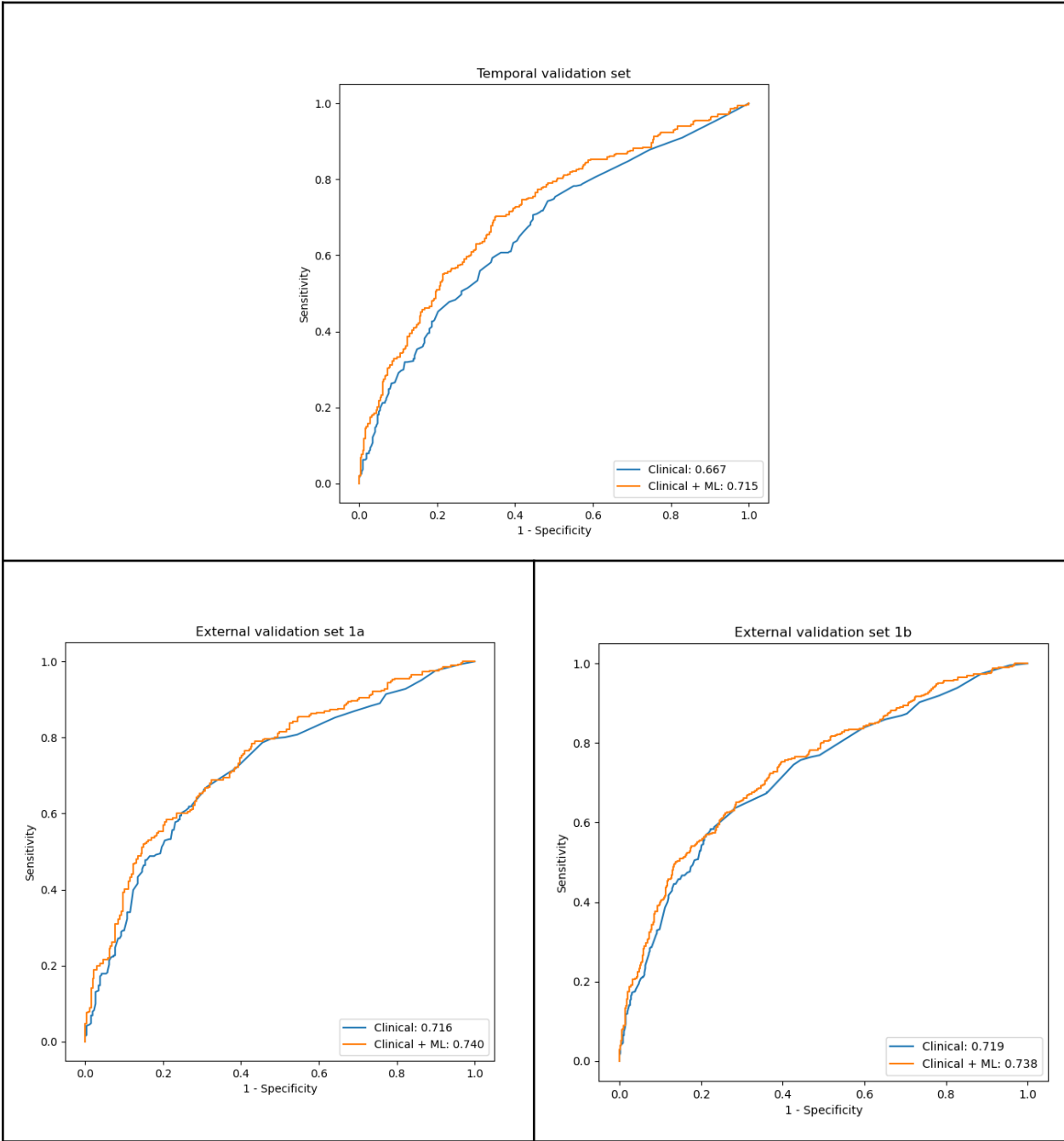
Model	Metric	Temporal validation	External validation 1a	External validation 1b
<b>Clinical</b>	Accuracy	62.4% [58.8, 65.8]	67.8% [64.0, 71.8]	67.8% [64.7, 70.7]
	Sensitivity	59.3% [54.0, 64.5]	66.3% [60.8, 71.7]	63.6% [58.8, 67.9]
	Specificity	65.8% [60.4, 70.9]	69.5% [63.6, 75.1]	71.8% [67.5, 75.4]
	PPV	66.0% [60.9, 71.1]	71.0% [65.4, 76.7]	67.4% [63.0, 71.8]
	NPV	59.1% [54.1, 64.3]	64.7% [58.9, 70.1]	68.2% [63.4, 72.2]
<b>Clinical + ML</b>	Accuracy	67.8% [64.0, 71.3]	68.2% [64.5, 72.2]	68.3% [65.2, 71.2]
	Sensitivity	70.1% [65.2, 74.8]	68.7% [63.5, 73.9]	65.0% [60.2, 69.4]
	Specificity	65.2% [59.6, 70.3]	67.6% [61.7, 73.0]	71.3% [67.2, 75.3]
	PPV	69.3% [64.5, 74.3]	70.4% [64.5, 75.4]	67.6% [63.3, 72.1]
	NPV	66.0% [60.6, 71.0]	65.8% [60.1, 71.6]	68.9% [64.2, 72.8]

**Supplementary Table S5: AUROC for LNM prediction without accounting for baseline clinicopathologic variables during machine-learned feature selection.**

AUROC for LNM predictions for logistic regressions with various feature sets. Clinical: baseline clinicopathologic variables (age, sex, tumor grade, T-category, lymphatic invasion, venous invasion). Clinical + ML: baseline clinicopathologic variables plus 5 machine-learned features selected without controlling for baseline clinicopathologic variables. 95% confidence intervals computed via bootstrapping.

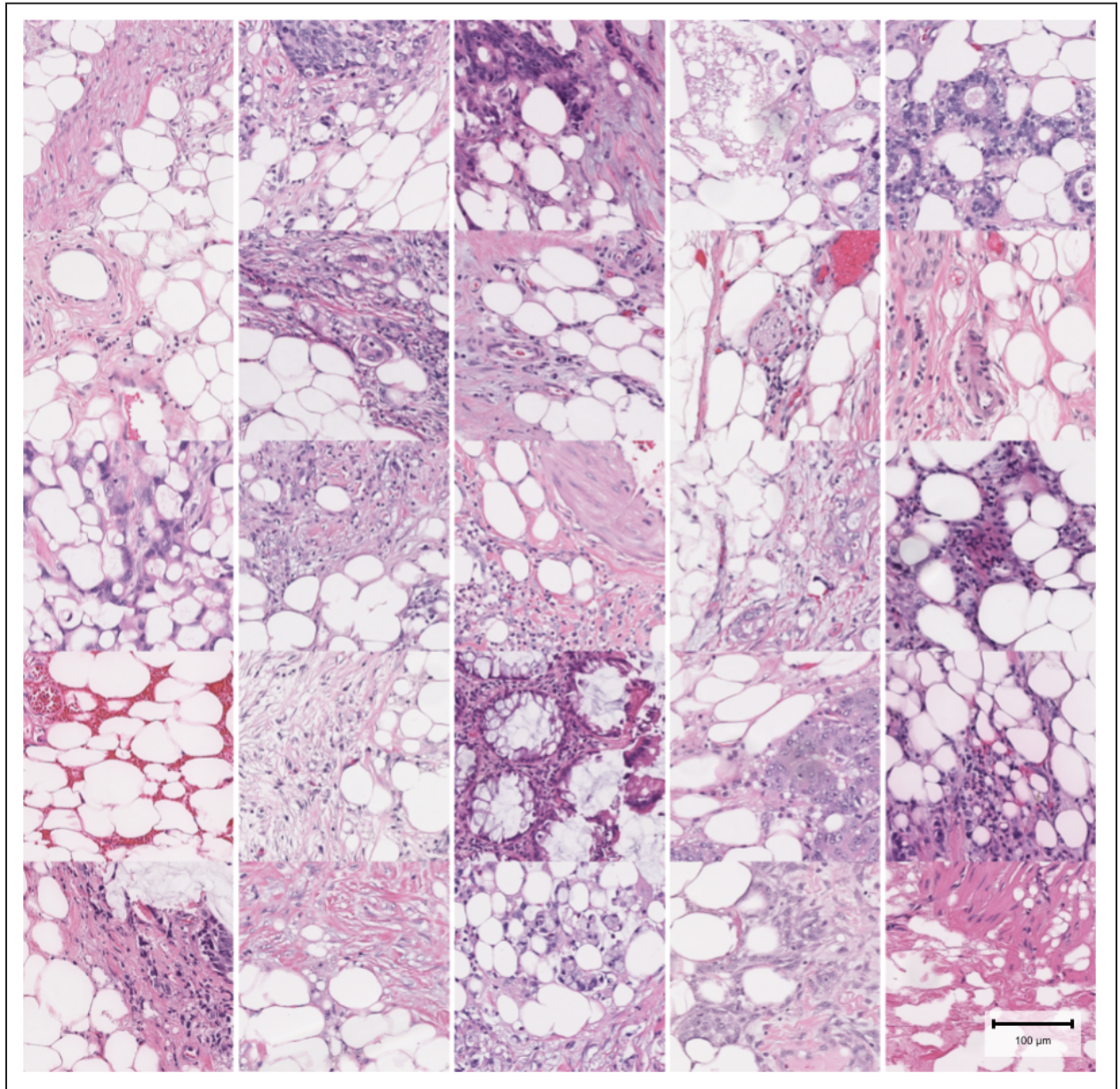
<b>Model</b>	<b>Temporal validation</b>	<b>External validation 1a</b>	<b>External validation 1b</b>
<b>Clinical</b>	0.667 [0.626, 0.708]	0.716 [0.674, 0.762]	0.719 [0.684, 0.752]
<b>Clinical + ML</b>	0.710 [0.669, 0.747]	0.706 [0.662, 0.750]	0.700 [0.666, 0.736]
<b>Delta</b>	0.042 [0.017, 0.070]	-0.010 [-0.039, 0.019]	-0.019 [-0.040, 0.002]

# Supplementary Figures

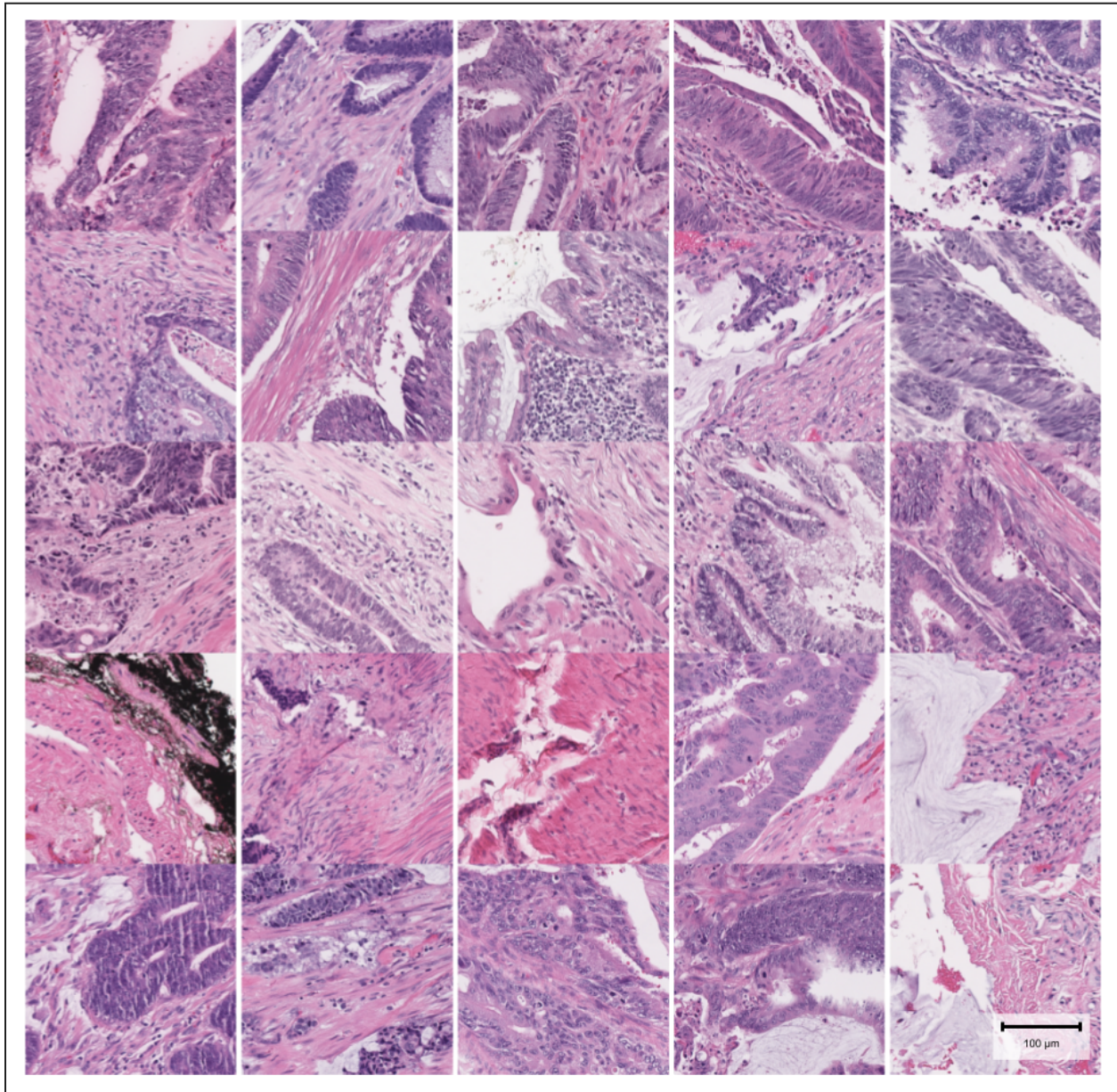


**Supplementary Figure S1: Receiver operating characteristic (ROC) curves for Clinical vs Clinical + ML prediction models on validation datasets.** ROCs with AUROCs for LNM predictions for logistic regressions with various feature sets. Clinical: baseline clinicopathologic variables (age, sex, tumor grade, T-category, lymphatic invasion, venous invasion). Clinical + ML: baseline clinicopathologic variables plus 5 machine-learned features.

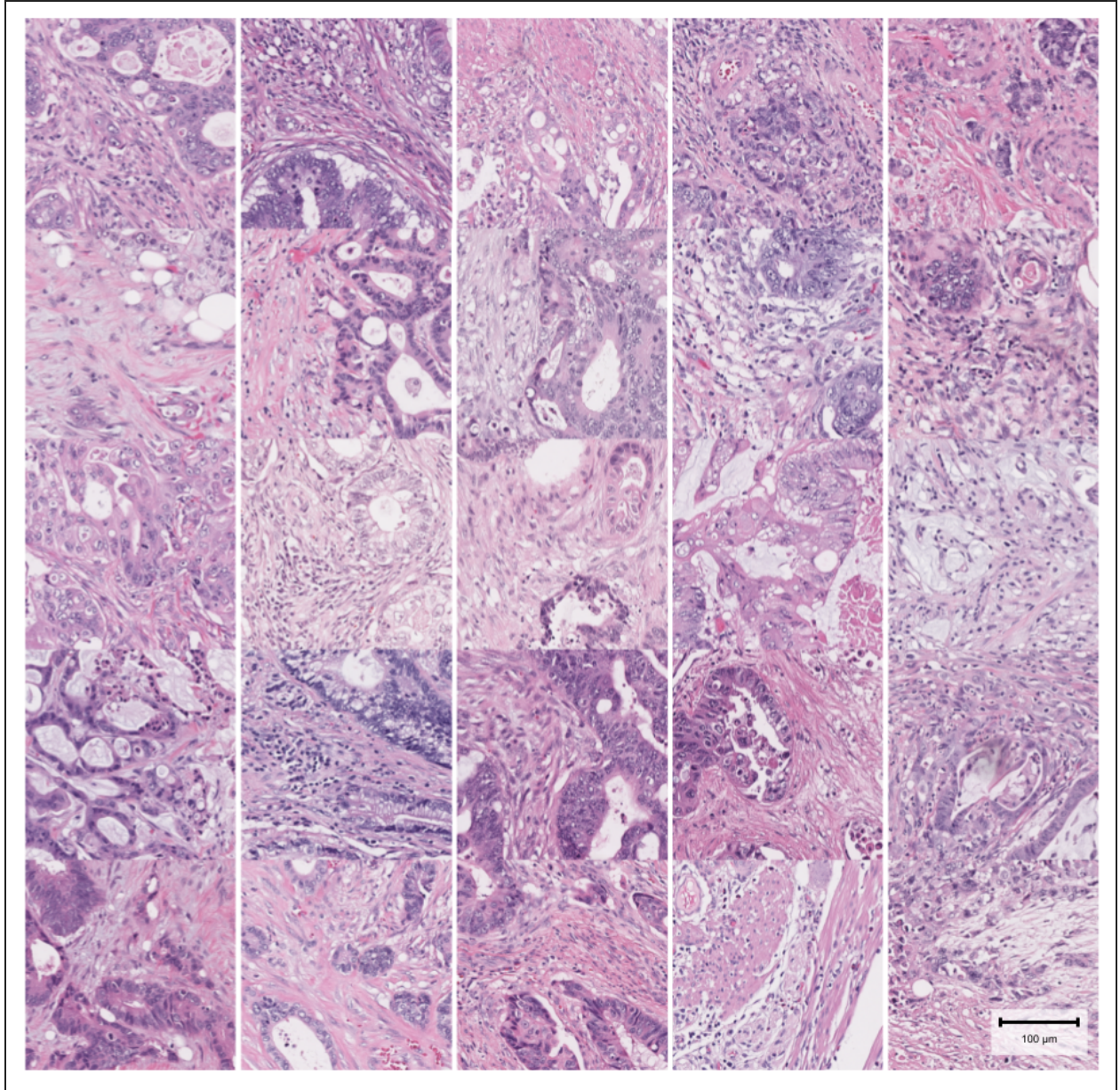




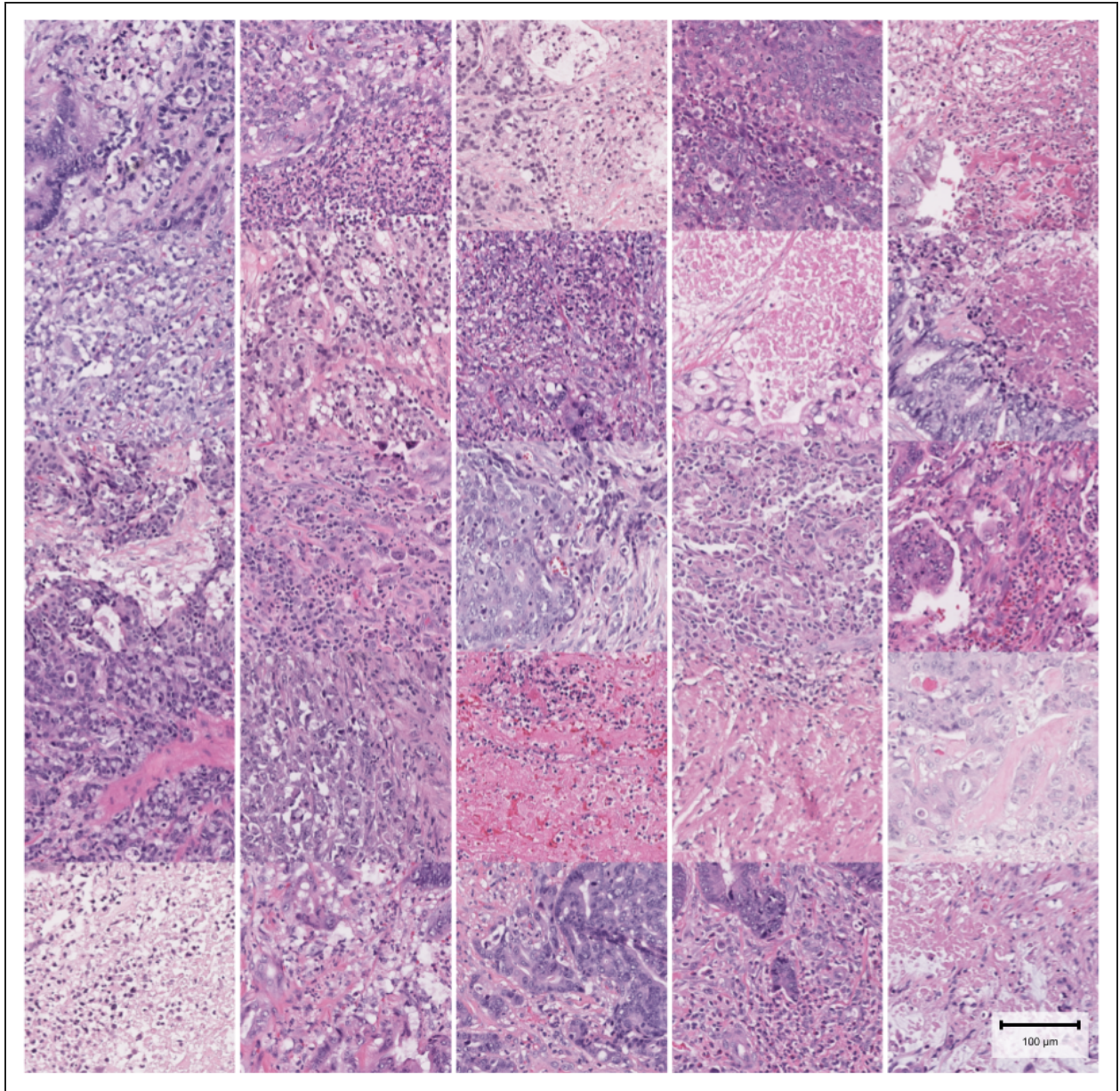
**Supplementary Figure S2: Additional patches assigned to machine learning feature #1 from external validation set 1a.** Patches selected here are the next 25 patches closest to the cluster centroid (after the five previously shown in Figure 2), and each patch is sampled from a unique case. Patches are 289x289 pixels obtained at 10X, with scale bar in lower right showing length of 100 micrometers.



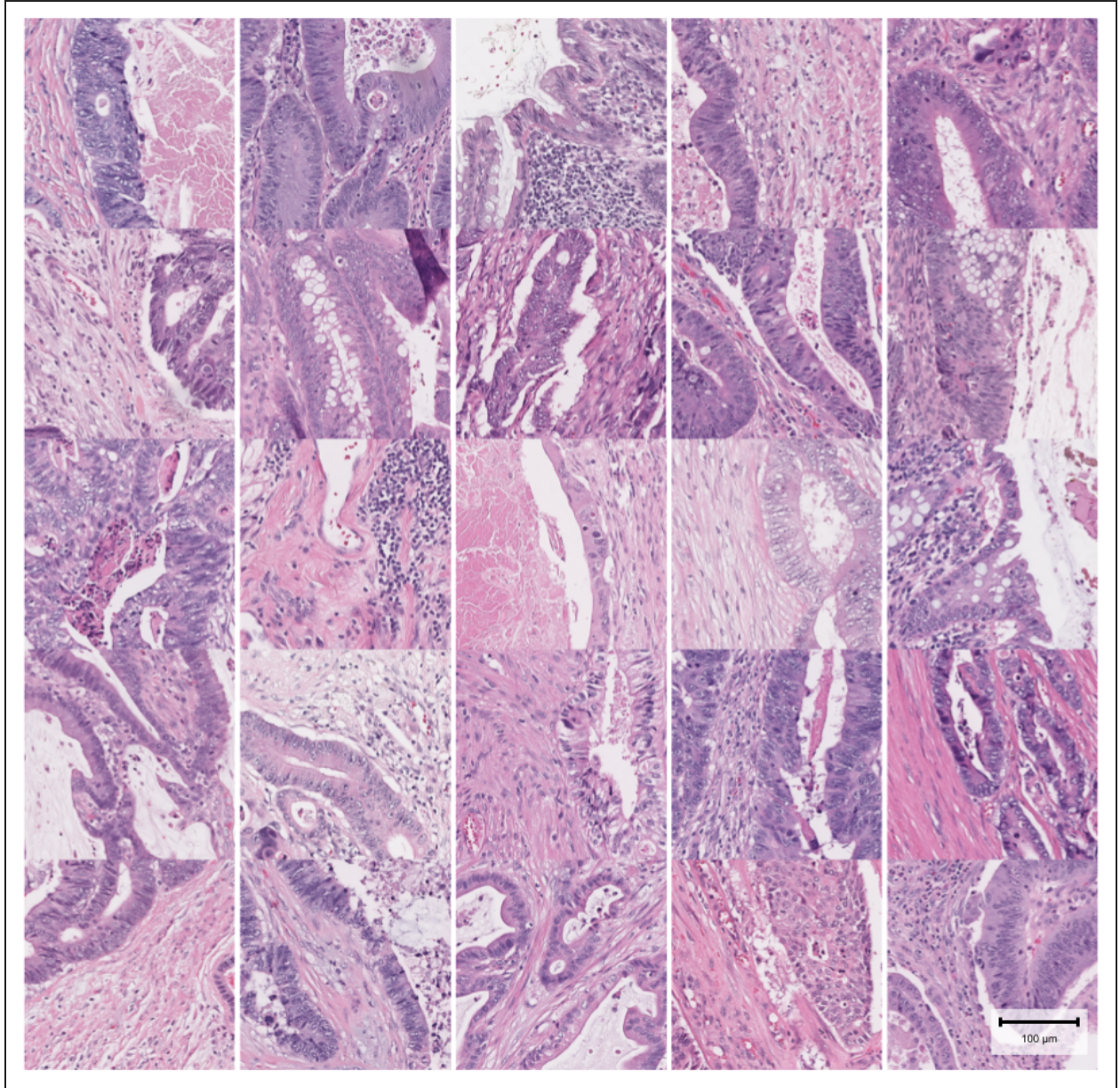
**Supplementary Figure S3: Additional patches assigned to machine learning feature #2 from external validation set 1a.** Patches selected here are the next 25 patches closest to the cluster centroid (after the five previously shown in Figure 2), and each patch is sampled from a unique case. Patches are 289x289 pixels obtained at 10X, with scale bar in lower right showing length of 100 micrometers.



**Supplementary Figure S4: Additional patches assigned to machine learning feature #3 from external validation set 1a.** Patches selected here are the next 25 patches closest to the cluster centroid (after the five previously shown in Figure 2), and each patch is sampled from a unique case. Patches are 289x289 pixels obtained at 10X, with scale bar in lower right showing length of 100 micrometers.

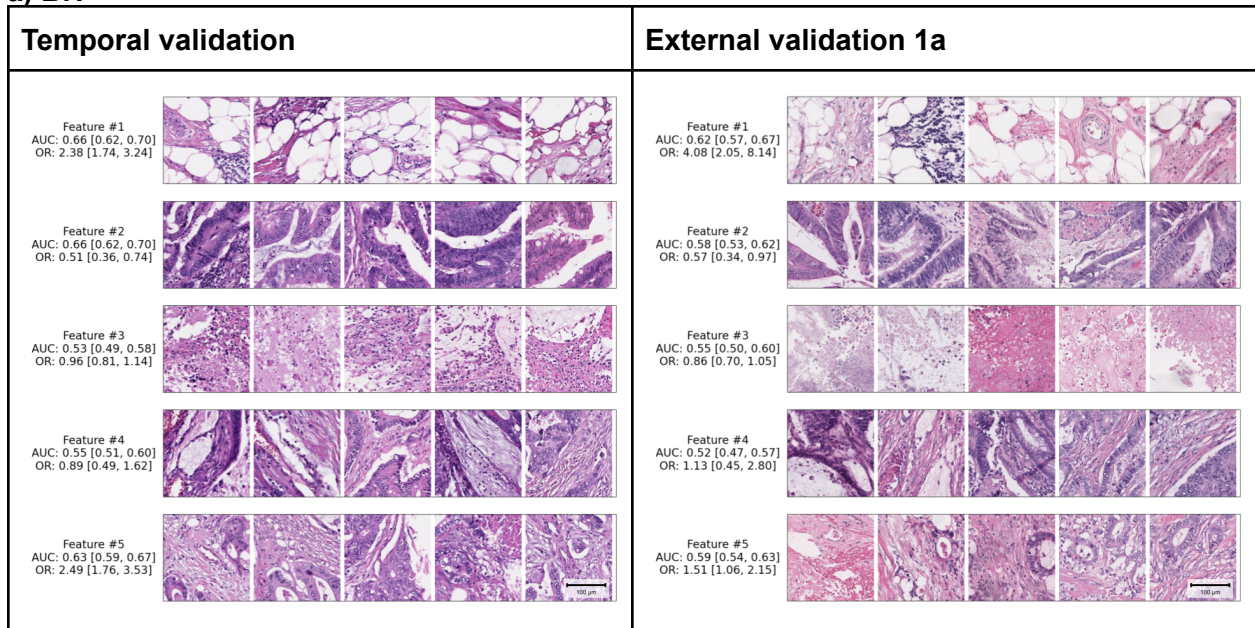


**Supplementary Figure S5: Additional patches assigned to machine learning feature #4 from external validation set 1a.** Patches selected here are the next 25 patches closest to the cluster centroid (after the five previously shown in Figure 2), and each patch is sampled from a unique case. Patches are 289x289 pixels obtained at 10X, with scale bar in lower right showing length of 100 micrometers.

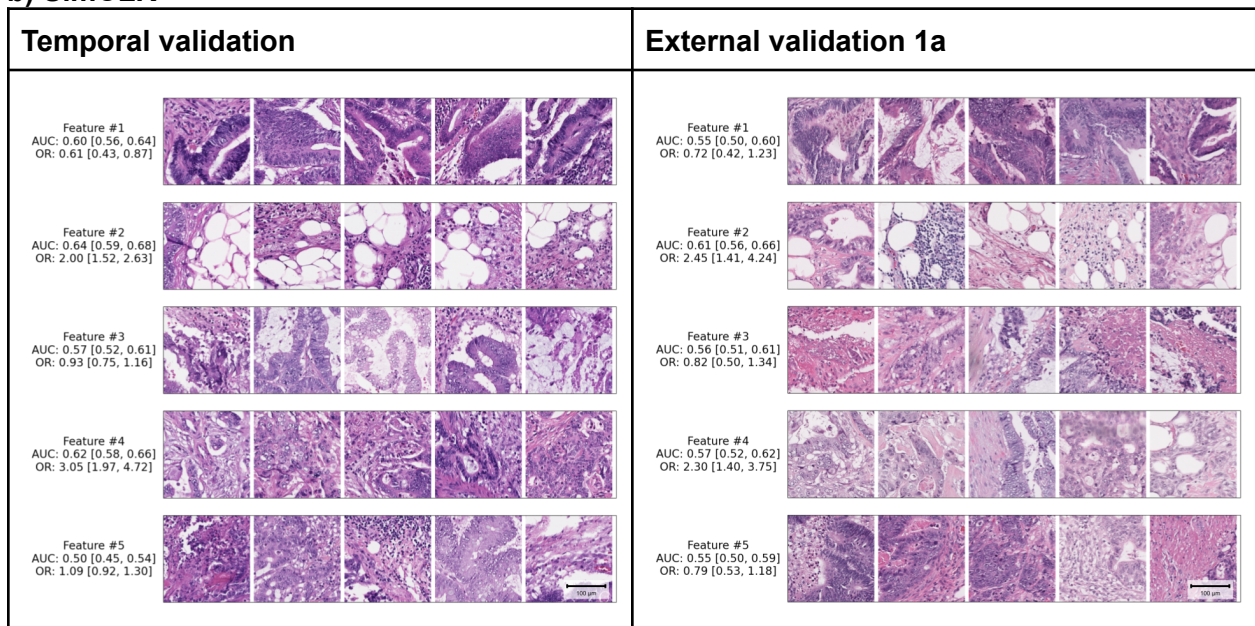


**Supplementary Figure S6: Additional patches assigned to machine learning feature #5 from external validation set 1a.** Patches selected here are the next 25 patches closest to the cluster centroid (after the five previously shown in Figure 2), and each patch is sampled from a unique case. Patches are 289x289 pixels obtained at 10X, with scale bar in lower right showing length of 100 micrometers.

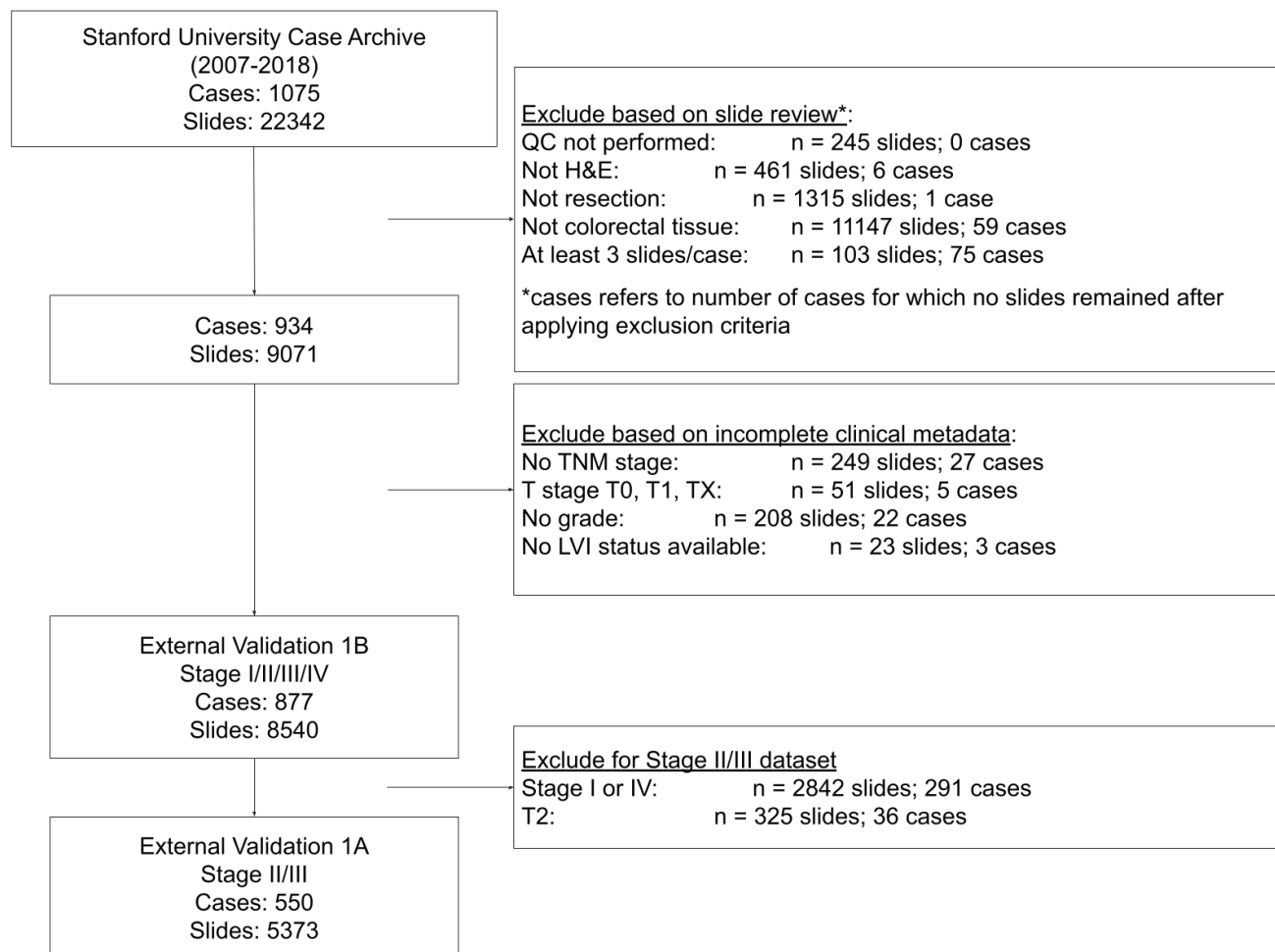
**a) BiT**



**b) SimCLR**



**Supplementary Figure S7: Machine-learned features for alternative embedding models**  
 Machine-learned features for temporal validation set selected using alternative embedding models: a) BiT and b) SimCLR. Patches are 224x224 pixels obtained at 10X, with scale bar in lower right showing length of 100 micrometers.



**Supplementary Figure S8: STARD diagram of inclusion/exclusion criteria for external validation data cohorts.**